Effect of Matric Suction on Permeability and Shear Strength of Vegetated Soils

Qi Liu[1,3], Lijun Su[1,2,3](✉), Chonglei Zhang[1], Bingli Hu[1,3], and Siyou Xiao[4]

[1] Key Laboratory of Mountain Hazards and Earth Surface Process, Institute of Mountain Hazards and Environment, CAS, Chengdu 610041, China

[2] China-Pakistan Joint Research Center on Earth Sciences, Islamabad 45320, Pakistan

[3] University of Chinese Academy of Sciences, Beijing 100049, China

[4] Liupanshui Normal University, Liupanshui 553000, China

Abstract. Matric suction is an important parameter to designate the mechanical properties of unsaturated soil. To explore the influence of matric suction on the properties of unsaturated soil covered by vegetation, a series of laboratory tests were conducted to investigate the effects of matric suction on the permeability and shear strength indexes in vegetated soils. 8 test boxes compacted with sandy silt were prepared, six of which were covered with *Cynodon dactylon* and *Indigofera amblyantha* while two boxes were left bare as control. The results showed that the water retention capacity of vegetated soil was significantly improved compared with the bare soil. The variations in water infiltration amount presented a similar trend with time in bare and vegetated soils, and the water infiltration amount of vegetated soil (Herbs) and vegetated soil (Shrubs) was about 1/2 and 2/3 of bare soil when infiltration time was 2 h, respectively. The permeability coefficient of bare and vegetated soils gradually decreased as matric suction increased, and the permeability coefficient of vegetated soils was obviously lower than bare soil. Permeability coefficient of vegetated soils decreased to the magnitude of 1.00E-08 when soil matric suction was about 25 kPa. According to the soil-water characteristic curve of sandy silt, shear strength indexes of bare soil and vegetated soils increased as matric suction augmented in the boundary effect region and the transition region. The rate of increase in soil cohesion slowly diminished, and internal friction angle increased gradually as the matric suction augmented. The consequences are of great significance for using vegetation to prevent slope instability and other geological disasters, meanwhile furtherly enriching the hydraulic mechanism of vegetation in slope stability.

Keywords: Vegetated soil · Matric suction · Soil-water characteristic curve · Permeability coefficient · Shear strength

1 Introduction

The interaction between soil and water is a major topic in the research field regarding slope engineering [1]. Rainfall infiltration can increase pore-water pressure of slope soil

H.-H. Zhu et al. (Eds.): BRWSG 2021, LNCE 230, pp. 44–59, 2022.
https://doi.org/10.1007/978-981-16-9963-4_4

mass, reduce the shear strength of the potential sliding surface of rock-soil mass, and then induce slope instability [2, 3].

Vegetative protection is an effective way to increase slope stability. In particular, for the shallow slopes with a depth of 1–2 m, plants can not only improve slope stability by root reinforcing but also dissipate the excess pore-water pressure in soil via root water uptake [4–6]. Moreover, plant transpiration induces soil matric suction can increase the shear strength of slope superficial soil [7, 8]. For cohesive slopes, vegetated soil can maintain the matric suction within 5–20 kPa in the root zone under one 10-year return period rainfall [9, 10] and the matric suction more than 9 kPa under one 100-year return period rainfall [10, 11].

As one of two independent variables which control the stress-strain characteristic of unsaturated soil [12], the variation of matric suction will induce the change of soil properties, such as permeability and shear strength [3, 13–15]. The influence of vegetation on the matric suction distribution in superficial soil reduces when rainfall intensity is high [16]. Plant roots could effectively limit the development of soil fissures, whereas straight roots also provided infiltration channels for rainfall and the dominant flow, which would increase soil permeability [17, 18]. However, plant roots occupied the soil pores, which could improve soil-water retention capacity and then reduce soil permeability coefficient [11, 19–22].

Matric suction also makes a significant contribution to the shear strength of unsaturated soil [1]. For unsaturated loess specimens, when matric suction is weak, the volumetric strain of specimens changes gradually from shear shrinkage to shear dilation. Soil cohesion increases with the advance of matric suction, and the change in internal friction angle is not obvious [23]. The cohesion of unsaturated reticulate red clay is more sensitive to matric suction change than the internal friction angle. As matric suction increases, the cohesion has an increasing trend followed by a reduction [24].

At present, researchers regarding unsaturated soil mainly adopt the methods of remodeling the samples to control soil water content, which does not take soil pore-water pressure into consideration, thus ignoring the influence of matric suction on soil shear strength in practice. At the same time, the impact of matric suction of vegetated soil on soil permeability characteristics is absent. Based on this, in this paper, sandy silt was selected as the carrier, and *Cynodon dactylon* and *Indigofera amblyantha* were chosen as tested plants. Soil homogeneity and the consistency of plants' growing environment were controlled. As a result, the influences of matric suction on permeability and shear strength of vegetated soils were studied so as to investigate the hydraulic mechanism of soil reinforcement and slope protection via vegetation.

2 Materials and Methods

2.1 Materials and Equipment

The soil samples used for testing were obtained from a cutting slope on the first phase urban expressway in Xiazhou avenue in Yichang, China, and were representative of sandy silt in this region. Tested soil was chosen below the surface of 0.3 m, and impurities in the soil were eliminated. The soil was air-dried, crushed and sieved through a 2.0 mm sieve. After that, soil particle size distribution was obtained from vibrating screens and

Malvern spray particle size analysis (Fig. 1). Table 1 presents several basic properties of the tested soil, such as specific gravity, optimum water content, pH value, plastic limit and liquid limit (Table 1).

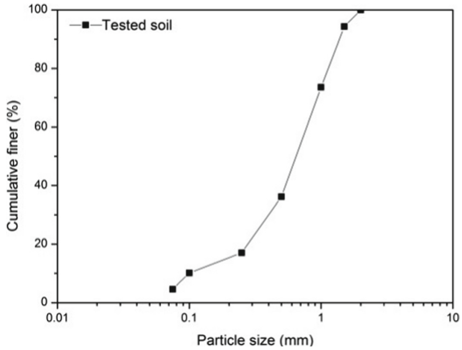

Fig. 1. Grain size distribution curve of tested soil

Table 1. Basic physical properties of experimental soil

SG	OMC (%)	MDD (%)	pH	LI (%)	PI (%)	SPC/m·s^{-1}
2.69	18.6	1.61	6.5	27.5	22.3	5.75×10^{-6}

Note: SG is specific gravity, OMC is optimum moisture content, MDD is maximum dry density, *LI* is a liquid limit, *PI* is the plastic limit, and *SPC* is saturated permeability coefficient.

Cynodon dactylon and *Indigofera amblyantha*, used widely in slope greening projects, were selected as test plants. *Cynodon dactylon* is a gramineae perennial herb, possess rhizomes and stolon. It can grow well in light sand and light acid-alkali land, as well as strong ability in drought resistance. Indigofera amblyantha belongs to a perennial deciduous shrub, and its growing period is 6 months approximately, possesses a strong ability in drought resistance and barren resistance. Both the two plants being mentioned above are the most common soil-water conservation plants in tropical and subtropical regions.

Soil permeation instrument: the WS-55 type permeation instrument produced by Nanjing Soil Instrument Co., Ltd in China was used in this paper. The sample size is Ø61.8 mm × 40 mm, and specimens were prepared according to the instructions in the Geotechnical Test Method Standard (GB/T50123–1999) in order to measure the soil permeability coefficient.

Direct shear apparatus: the ZJ strain-controlled four-type direct shear instrument was employed in this paper, produced by Nanjing Soil Instrument Co., Ltd in China. The instrument with a maximum vertical load of 400 kPa, and the sample size is Ø61.8 mm × 20 mm. Shear velocities including 2.4, 0.8, 0.1 and 0.02 mm/min, respectively.

Mini-lysimeter: the instrument is a SoilTron automatic weighing lysimeter, which consists of the multi-layer profile detectors and the data collector. The plants were cultivated in a woody cubic box. In the front surface of the box, several holes were set orderly from top to bottom so that detectors could be inserted to measure soil matric suction. Moreover, the data collector was utilized to automatically collect and record the data of each detector regularly.

2.2 Test Design and Methods

The size of the woody cubic box is 300 mm × 300 mm × 300 mm. Homogeneous soil through a 2 mm sieve was placed in the box, soil height and compactness were 250 mm and 90%, respectively [10, 25]. For both *Indigofera amblyantha* and *Cynodon dactylon*, three replicates each were set. In addition, four bare replicates were prepared as comparisons. In the planting experiment, the planting density of *Cynodon dactylon* was 15 g/m^2, while which of *Indigofera amblyantha* was 80–100 plants per square meter [25, 26].

The planting experiment was conducted in an open space behind a laboratory in China, Three Gorges University. After spreading plant seeds, planting samples were watered completely. All planting samples were subjected to the same conditions of rainfall, temperature and light. The planting period of *Cynodon dactylon* was half a year, while which of *Indigofera amblyantha* was 2 years (Fig. 2).

Fig. 2. Planting experiment

Transpiration Test. The transpiration test was conducted in a laboratory in China, Three Gorges University. The laboratory was set at a temperature of 20 °C ± 2 °C, a humidity of 50%–60%, an illumination height of 1m, cold light illuminator (plant growth lamp) is 36 W, and thermal light illuminator is 275 W [10, 27].

A pair of 5 mm diameter holes were set from top to bottom every 50 mm on the planting box. Then detectors of lysimeter were inserted into the holes to measure soil matric suction. The planting samples were uniformly watered before conducting the test until accumulated water occurred on the surface of the samples. Subsequently, a drying test (soil evaporation or plant transpiration) was performed, and the variations of matric suction at 5 cm, 10 cm, 15 cm and 20 cm depth were monitored automatically once every 10 min through the lysimeter (Fig. 3).

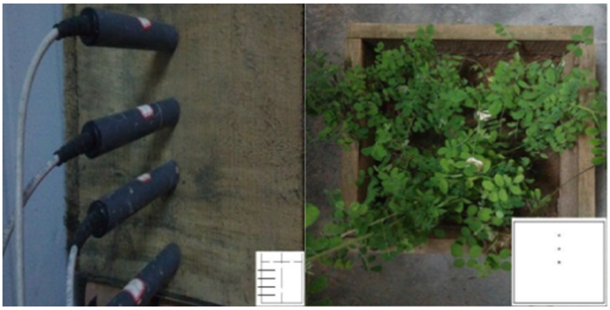

Fig. 3. Transpiration test

Direct Shear Test. After the drying test was completed, the above-ground biomasses of planting samples were eliminated, and the planting box was disassembled. Specimens were taken horizontally at different depths of the center of the samples by using the cutting ring, which matched with the direct shear instrument. Twenty cutting-ring specimens were taken at the same depth, and consistent root biomass was ensured. Five groups of specimens were set, with four cutting-ring specimens in each group. Each set of specimens was humidified or dried, and the matric suction was controlled by 5 kPa, 10 kPa, 15 kPa, 20 kPa and 25 kPa, respectively.

Considering the confining pressure on vegetated soil in the actual practice, the cutting-ring specimens were loaded under the normal stress of 25 kPa, 50 kPa, 75 kPa and 100 kPa and sheared at the rate of 0.02 mm/min until the readings of the dynamometer do not change with the increase of shear displacement (Fig. 4). In the shear test, the maximum shear stress under each vertical load was obtained [28].

Fig. 4. Direct shear test

The test results were plotted in a τ-P curve, and then the cohesion c and the internal friction angle φ of specimens were obtained. The relationship between shear stress and normal stress can be expressed by the followed formula:

$$\tau = c + p \tan \varphi \tag{1}$$

where τ is the shear stress of specimens, kPa; c is the cohesion, kPa; φ is the internal friction angle, °; p is the normal stress, kPa.

Fig. 5. Penetration test

Penetration Test. The sampling procedures were the same as the direct shear test. Matric suction of cutting-ring specimens within the same group was kept the same, and the ones with a large difference in matric suction were humidified or dried. The permeability coefficient of bare soil, vegetated soil of *Indigofera amblyantha* and *Cynodon dactylon* were measured by the constant head penetration test, with a duration time of 2 h.

Porous stone and sealing ring was set into the base of the permeation instrument, and then Vaseline was applied on the inner wall of the sleeve. The in-situ cutting-ring specimens were put into the permeation instrument and arranged on the base. The sealing ring, porous stone, upper cap, and tighten screw were arranged on the permeameter in a row to avoid leaking of air and water. The inlet pipe was connected to the water supply device, and then the permeameter was laid flat to ensure water and air venting. After water overflowed from the outlet pipe, the measurement was started. During the test, the water head tube was filled with water to the required height, then the tube clamp was closed, and the stopwatch was started. Meanwhile, the initial water head h_1 at the moment t_1 was measured. After the seepage was stable, the final water head h_2 at the moment t_2 was also recorded. Water temperatures at the beginning and end of the test were measured (Fig. 5).

$$k = 2.3\frac{aL}{A(t_2 - t_1)}log\frac{h_1}{h_2} \tag{2}$$

where a- cross-sectional area of the head pipe, cm^2; L-sample height, cm; A-cross-sectional area of the sample, cm^2; h_1-initial water head (t_1), cm; h_2-final water head (t_2), cm. In this test, the cutting-ring sample has a cross-sectional area of 30 cm^2 and a height of 40 mm.

3 Results and Discussion

3.1 Soil-Water Characteristic Curve

In recent years, a large number of empirical models have been proposed to describe the properties of soil-water characteristic curves. For example, Brooks-Corey, Fledlund-Xing and Van-Genuchten models of which fitting parameters were obtained based on experimental observations [29–31]. According to the soil-water characteristic curve, as matric suction of unsaturated soil increased, the soil saturation decreased with several recognizable phrases. The matric suction can be divided into three regions according to the tangent slope of the soil-water characteristic curve, namely, the boundary effect region, the transition region and the unsaturated residual region, where the transition region can be further subdivided into primary and secondary transition regions [32].

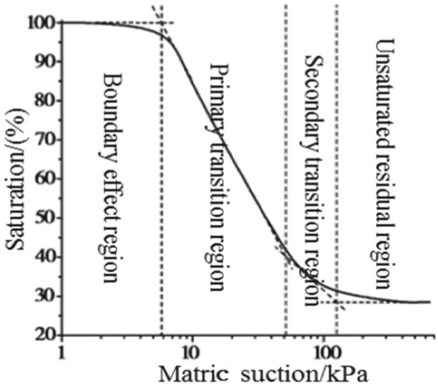

Fig. 6. The typical soil-water holding capacity curve [33]

Through pressure plate test, the water retention capacity curve of unsaturated remolded loess can be divided distinctly into four sections. And turning point values of the boundary effect region, the primary transition region, the second transition region and the unsaturated residual region were around 5 kPa, 60 kPa and 170 kPa, respectively (Fig. 6) [33]. Based on the viewpoint that plant roots occupy soil particle gaps and reduce soil porosity, the void ratio of vegetated soil was deduced via the three-phase diagram of soil [8]:

$$e = \frac{e_0 - R_v(1 + e_0)}{1 + R_v(1 + e_0)} \tag{3}$$

where e_0-the void ratio of bare soil, R_v-the volume ratio of plant roots.

A numerical model regarding soil saturation and soil matric suction was established so as to simulate the effect that plant roots reduce soil porosity and increase soil-water retention capacity [20]:

$$S_r = \left[1 + \left[\frac{se^{m_4}}{m_3}\right]^{m_2}\right]^{-m_1} \tag{4}$$

where S_r-the soil saturation; s-soil matric suction; m_1, m_2 and m_4 are dimensionless parameters; m_1 and m_2 control the basic shape of the soil-water characteristic curve; m_3 and m_4 are related to the intake value of bare soil.

In this paper, computed conclusions showed that the average void ratio (e_0) of bare soil is 0.558, whereas which of vegetated soil (*Indigofera amblyantha*) is 0.536. Through the compacted kaoline test, the recommended values of $m_1 = 0.03586$ and $m_2 = 3.746$ were offered [34, 35]. Based on the soil-water characteristic curve of sandy silt, $m_3 = 37.161$ kPa and $m_4 = 8.433$ kPa were employed to carry out a numerical simulation for bare soil [36–38]. In addition, 5 groups date of vegetated soil were verified, and the results were demonstrated in Fig. 7.

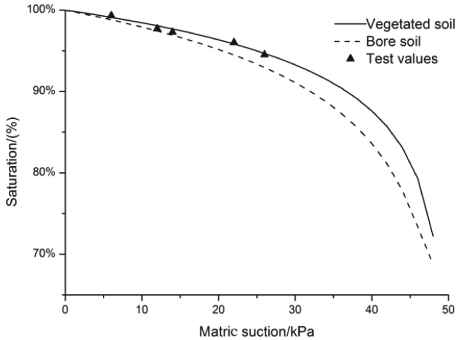

Fig. 7. Water holding capacity of bare soil and vegetated soil (Sandy silt)

Figure 7 showed that the equation of soil matric suction and soil saturation established by Gallipoli et al. [20] could effectively simulate the experimental data with high accuracy. The water retention capacity of vegetated soil is higher than that of bare soil, but the water retention capacity curves of those two are similar. This indicates that plant roots in vegetated soil can effectively increase the air intake value of soil but do not have much influence on the rate of change in soil water content.

During the plant growth period, soil particles were arranged in a definite direction and order under gravity stress, and a certain pore structure was formed [39–41]. During the drying process of soil, gas initially entered the pores with a large size and drained the pore water in soil pores. This part of pore water accounts for a large proportion of the total pore water. As soil matric suction increase, the water in soil pores decrease gradually, non-pore water is drained slowly, and soil presents a high water retention capacity. Plant roots in the vegetated soil can effectively fill the pores among soil particles, and soil porosity is lowered. During the drying process of vegetated soil, it is difficult for gas to enter the gaps of soil particles. Thus air intake value of the vegetated soil is higher than which of the bare soil.

3.2 Permeability Coefficient

As shown in Fig. 8, the amounts of water permeation of both vegetated soil and bare soil increased gradually with a similar variation tendency during the process of the penetration test. When the duration time of penetration test was 2 h, the amount of water infiltration of vegetated soil of *Cynodon dactylon* was about 1/2 of that of the bare soil, whereas which of *Indigofera amblyantha* was around 2/3, which indicated that vegetated soil could effectively reduce soil penetration rate. The permeation rate of both vegetated soil and bare soil presented a gradual decline tendency and reached a stable seepage state. However, the permeation rate of vegetated soil was always lower than that of bare soil.

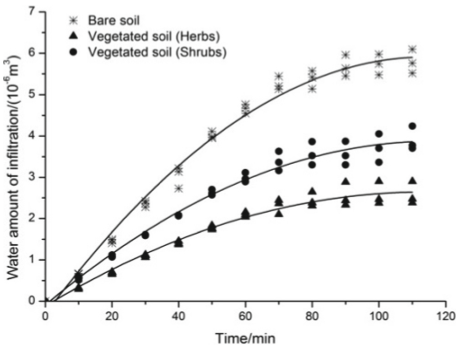

Fig. 8. Variations of the amount of water infiltration in different soils

Results could be explained by plant roots exerting growing pressure on the surrounding soil during the plant growing process, soil relative density increase and void ratio decrease [8, 41]. Lots of bifurcations and fibrous roots can promote soil consolidation and improve soil structure by network connecting and twining, and then the cohesion and friction force between soil particles and plant roots is increased. Meanwhile, the cementing materials produced by biochemical actions between plant roots and soil particles, the organic and inorganic colloids such as cationic bridges and Van der Waals forces formed through multivalent cations in the soil, all those mentioned above can combine soil and root system into an organic complex. Therefore, the integrity of soil is improved, and the penetration rate of soil decreases.

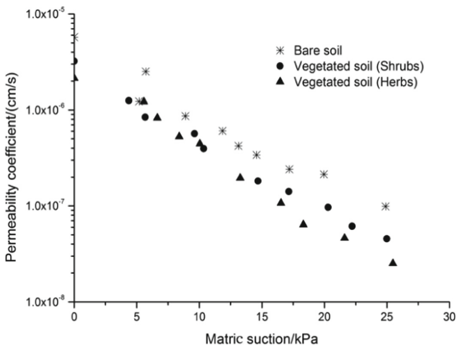

Fig. 9. Relation between soil matric suction and permeability coefficient

The relationship between permeability coefficient and matric suction of vegetated soil and bare soil can be observed in Fig. 9. The permeability coefficient of specimens decreased gradually with the advance of matric suction, and the permeability coefficient of vegetated soil is significantly lower than that of bare soil. In unsaturated soil, pore water is a hydrophilic medium, and air is a hydrophobic medium, so water can only flow through the space occupied by pore water. When matric suction is augmented, the soil moisture content is decreased. Furtherly, the soil permeability coefficient is reduced correspondingly. When the matric suction of vegetated soil is 25 kPa, the permeability coefficient is reduced to the magnitude of 1.00E-08. That indicated the increase in soil pore air pressure impeded the paths of water flow, which reduced the permeability of vegetated soil.

The permeability coefficient of bare soil is higher than that of vegetated soil. In the process of rainfall, the variation of matric suction in vegetated soil is mild, resulting in a longer response time and thereby presumably to a greater soil shear strength in the corresponding period.

3.3 Shear Strength

Figure 10 illustrated that under different normal stresses, the shear strength of bare soil and vegetated soil increase with the advance of matric suction, and the various characteristics of shear strength are almost the same. This manifests that matric suction can be regarded as an independent variable in the shear strength of unsaturated soil. Moreover, two relationship curves show a correlation and both all have significant phases. One is about soil shear strength and matric suction, and the other is about soil saturation and matric suction.

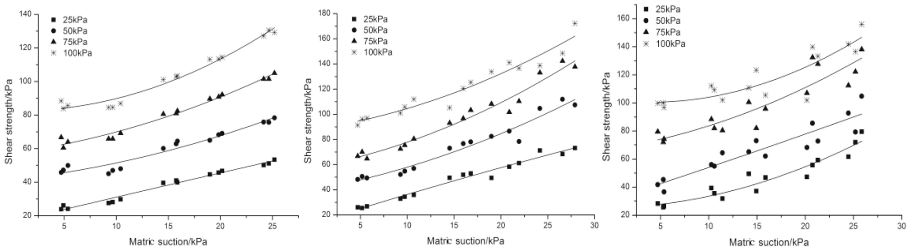

a) Bare soil b) Vegetated soil (Herbs) c) Vegetated soil (Shrubs)

Fig. 10. Relationship between shear strength and matric suction of unsaturated sandy silt

According to Fig. 6, there are four significant phases in the soil-water characteristic curve of unsaturated soil. The matric suction of specimens in this paper is mainly concentrated in the boundary effect zone and the main transition zone. The slope turning point of the soil-water characteristic curve regarding sandy silt in Fig. 7 and the slope turning point of the relationship curve between shear strength and matric suction in Fig. 10a are almost the same, which is the air intake value of saturated sandy silt. In Fig. 10b and Fig. 10c, when the normal stresses are low, the slope variation of the relationship curve between shear strength and matric suction of vegetated soils (Herbs and Shrubs) is small, even remaining stable until matric suction is 25 kPa. According to the soil-water characteristic curve (Fig. 7) of vegetated soil and the shear strength variation characteristics of bare soil, it is straightforward to conclude that compared with bare soil, the air intake value of vegetated soil is higher.

It can be obtained from Fig. 10 that soil shear strength increase due to an increase in matric suction. The Least Square method was adopted to fit the data, and the results were summarized in Table 2.

Table 2. Regression equation of shear strength and matric suction under different normal stresses

Soil type	Normal stress/kPa	Regression equation	R2	n
Bare soil	25	$\tau = 0.0047S^2 + 1.3012S + 17.48$	0.981	15
	50	$\tau = 0.0353S^2 + 0.6046S + 41.21$	0.936	15
	75	$\tau = 0.0472S^2 + 0.6902S + 57.92$	0.979	15
	100	$\tau = 0.0841S^2–0.1156S + 82.01$	0.972	15
Vegetated soil (Herbs)	25	$\tau = -0.0073S^2 + 2.3454S + 13.55$	0.973	15
	50	$\tau = 0.0432S^2 + 1.3682S + 39.93$	0.953	15
	75	$\tau = 0.0582S^2 + 1.4022S + 57.94$	0.963	15
	100	$\tau = 0.0562S^2 + 1.0845S + 88.09$	0.937	15
Vegetated soil (Shrubs)	25	$\tau = 0.1009S^2–0.8960S + 102.59$	0.774	15
	50	$\tau = 0.0141S^2 + 1.8230S + 64.82$	0.924	15
	75	$\tau = 0.0307S^2 + 0.4975S + 52.19$	0.874	15
	100	$\tau = 1.6743S + 18.09$	0.971	15

It can be observed in Table 2 that under different normal stresses, the correlation coefficient value of shear strength and matric suction of bare soil was higher than 0.936 ($R^2 > 0.936$), whereas the correlation coefficient values of herbs vegetated soil and shrubs vegetated soil were more than 0.937 and 0.774 ($R^2 > 0.937$ and $R^2 > 0.774$), respectively. The difference could be explained by the shear strength of vegetated soil being related not only to matric suction but also to mechanical reinforcement induced by plant roots. Due to the difference in root amounts in each specimen varying from one to one when the specimens of vegetated soil were obtained through cutting-ring, the deviation may have occurred in the results. Based on this, on the same matric suction, three specimens were taken by cutting-ring for data statistics and fitting, which could reduce the bias of the results.

From Fig. 10, the cohesion and the internal friction angle of bare soil and vegetated soil both increased as matric suction increased. However, the rate of increase in cohesion decreased, and the internal friction angle increased. The soil-water characteristic curve can be divided into four phases according to Fig. 6, so the matric suction of specimens in this paper is mainly concentrated in the boundary effect region and the primary transition region.

The cohesion of sandy silt is mainly induced by the capillary action of pore water in the soil, and capillary action mainly occurs in the transition region of the soil-water characteristic curve [15]. When soil matric suction value locates in the boundary effect zone of the soil-water characteristic curve, the soil is almost saturated, and few gases within the soil are surrounded by pore water. In this situation, the water-gas system belongs to the gas seal system. The surface tension of the water-air interface shrink membrane in the gas seal system didn't apply to soil particles directly, nor did any obvious cohesion is induced [13, 14]. In addition, lubrication among soil particles is significant due to soil particles are surrounded by pore water. As a result, the variation magnitude of the internal friction angle at this phase is small.

The soil condition begins transforming from saturated to unsaturated in the transition region, air starts entering the soil pores, and the water-air interface shrinkage membrane begins to enlarge. The surface tension of the shrinkage membrane acts inversely on soil particles, and compressive stress is generated, and then soil cohesion increase. At the same time, as the soil was under an incompletely saturated condition, few gases occurred in soil micro-pores. Matric suction generated in soil micro-pores can effectively combine soil particles together, and lubrication among soil particles drops comparatively. In addition, both the soil cohesion and internal friction angle began to increase [42].

When matric suction continues to increase, the pore water in the soil decrease gradually, and a large quantity of gas enter the soil pores. The shrinkage membrane of the water-air interface in the soil pores declines correspondingly, and the total compressive stress act on soil particles decreases slightly, which results in the rate of increase in cohesion slowly dropping. The increased amplitude of internal friction angle increases as the lubrication diminishes and frictional resistance augments among soil particles [43].

As shown in Table 3, as the matric suction of bare soil advanced, the cohesion increased from 5.708 kPa to 25.779 kPa and the internal friction angle developed from 37.013° to 45.905°. By contrast, the variation amplitude of the internal friction angle was relatively small. The cohesion increment of herbs vegetated soil was 34.995 kPa, and the variation range of the internal friction angle was 44.872° ± 3.005°. Moreover, the cohesion increment and the internal friction angle variation range of shrubs vegetated soil were 24.678 kPa and 46.119° ± 2.964°, respectively. Based on the mentioned above, this might lead to the conclusion that compared with bare soil, herbs have a greater influence on the soil cohesion, while shrubs are weighed more on soil internal friction angle. The specimens were obtained in situ at side-by-side locations, but the results may have been influenced by in situ heterogeneity and possible differences in root amounts.

The results may be explained in another way. The root system of *Cynodon dactylon* can be characterized by luxuriant fibrous roots ($d < 1.0$ mm), with no strong taproot [44]. Indigofera amblyantha with a horizontal developed root system, including a lot of the branches and fibrous roots, and the root diameter is mainly concentrated in 1.0–2.5 mm [45].

Jackson believed that the roots with a diameter <2.0 mm are the principal organ for plants to uptake water [46]. Owing to the large surface area, the increase in connect area between fibrous roots ($d < 2.0$ mm) and soil particles intensified the permeability of root epidermis and water transmission tunnels. Whereas the roots of which diameter is greater than 2.0 mm, liquid water inside the roots is easily vaporized under high negative pressure to generate cavitation. The decline in the channels in which liquid

Table 3. Cohesion and internal friction angle of soil under different matric suction

Soil type	Shear strength indexes	5 kPa	10 kPa	15 kPa	20 kPa	25 kPa
Bare soil	Cohesion/kPa	5.708	10.081	19.799	21.838	25.779
	Internal friction angle/◦	37.013	38.365	39.485	42.642	45.905
Herbs vegetated soil	Cohesion/kPa	3.330	8.543	26.824	28.912	38.325
	Internal friction angle/◦	41.867	42.704	43.495	46.873	47.876
Shrubs vegetated soil	Cohesion/kPa	4.915	11.931	20.898	28.854	29.593
	Internal friction angle/◦	43.155	43.392	43.852	45.102	49.082

water flows results in lower soil permeability, and plant roots play a role in mechanical reinforcing soil. The root system of *Cynodon dactylon* can improve soil structure by cementing, consolidating soil, and dissipating pore water pressure. Whereas the root system of Indigofera amblyantha presents work in friction effect of soil-root interface and mechanical reinforcement effect. As a result, *Cynodon dactylon* (Herbs) may impact soil cohesion, and *Indigofera amblyantha* (Shrubs) has a significant influence on soil internal friction angle.

4 Conclusions

Through transpiration, penetration and direct shear tests, in this paper, the effects of matric suction on the permeability and shear strength of vegetated soil were investigated. The main findings can be summarized as follows:

(1) According to the results of the vegetative test and the water retention capacity curve of sandy silt, the wilting coefficients of *Cynodon dactylon* and *Indigofera amblyantha* corresponding to the matric suction of sandy silt is 35–40 kPa. To ensure the tests were conducted normally, the matric suction of specimens was maintained within 30 kPa, which is located in the boundary effect region and the initial stage of the transition region.
(2) Compared with bare soil, the water retention capacity of vegetated soil significantly improved. When the duration time of the penetration test is 2 h, the amount of water infiltration of vegetated soil of *Cynodon dactylon* was about 1/2 of that of the bare soil, whereas which of *Indigofera amblyantha* was around 2/3. Permeability coefficient of vegetated soil decreased to the magnitude of 1.00E-08, when soil matric suction was about 25 kPa.
(3) The rate of increase in soil cohesion slowly diminished and internal friction angle increased gradually as the matric suction augmented. Compared with bare soil, *Cynodon dactylon* (Herbs) impact more on soil cohesion and *Indigofera amblyantha* (Shrubs) has a significant influence on soil internal friction angle.

Acknowledgments. This study was financially supported by the National Natural Science Foundation of China (Grant No. 41790432), NSFC Key Project for International Cooperation (Grant

No. 41761144077), the International Partnership Program of Chinese Academy of Sciences (131551KYSB20180042) and the Youth Innovation Promotion Association CAS (Grant No. 2019364). Great appreciation also goes to the editorial board and the reviewers of this paper.

References

1. Wu, J.J., Wang, C.H., Li, G.X.: Influence of matric suction in unsaturated soils on slope stability. Rock Soil Mech. **25**, 732–743 (2004)
2. Ng, C.W.W., Shi, Q.: A numerical investigation of the stability of unsaturated soil slopes subjected to transient seepage. Comput. Geotech. **22**, 1–28 (1998)
3. Zhan, T.L.T., Ng, C.W.W., Fredlund, D.G.: Field study of wetting infiltration into a grassed unsaturated expansive soil slope. Can. Geotech. J. **44**, 392–408 (2007)
4. Barker, D.H.: Vegetation and Slopes: Stabilization, Protection, and Ecology. Thomas Telford Press, London (1995)
5. Simon, A., Andrew, A., Collison, J.C.: Quantifying the mechanical and hydrologic effects of riparian vegetation on streambank stability. Earth Surf. Proc. Land. **27**, 527–546 (2002)
6. Normaniza, O., Barakbah, S.S.: Parameters to predict slope stability-soil water and root profiles. Ecol. Eng. **28**, 90–95 (2006)
7. Pollen-Bankhead, N., Simon, A.: Hydrologic and hydraulic effects of riparian root networks on streambank stability: is mechanical root-reinforcement the whole story? Geomorphology **116**, 353–362 (2010)
8. Ng, C.W.W.: A tmosphere-plant-soil interactions: theories and mechanisms. Chinese J. Geotech. Eng. **39**, 1–47 (2017)
9. Macneil, D.J., Steele, D.P., McMahon, W., Carder, D.R.: Vegetation for slope stability-prepared for quality services, civil engineering, highways agency. TRL Report Press, Berkshire (2001)
10. Ng, C.W.W., Woon, K.X., Leung, A.K., Chu, L.M.: Experimental investigation of induced suction distribution in a grass-covered soil. Ecol. Eng. **52**, 219–223 (2013)
11. Ng, C.W.W., Leung, A.K., Woon, K.X.: Effects of soil density on grass-induced suction distributions in compacted soil subjected to rainfall. Can. Geotech. J. **51**, 311–321 (2014)
12. Woon, K.X., Leung, A.K., Ng, C.W.W., Chu, L.M.: Effects of grass transpiration on suction induced in near-saturated soil condition. In: Mancuso, C., Jommi, C., D'Onza, F. (eds) Unsaturated Soils: Research and Applications. Springer, Heidelberg (2012). https://doi.org/10.1007/978-3-642-31343-1_30
13. Bishop, A.W., Blight, G.E.: Some aspects of effective stress in saturated and partly saturated soils. Géotechnique **13**, 177–197 (1963)
14. Fredlund, D.G., Morgenstern, N.R.: Stress state variables for unsaturated soils. J. Geotech. Eng. Division **103**(5), 447–466 (1977)
15. Lin, H.Z., Li, G.X., Yu, Y.Z., Lv, H.: Influence of matric suction on shear strength behavior of unsaturated soils. Rock Soil Mech. **28**, 1931–1936 (2007)
16. Lim, T.T., Rahardjo, H., Chang, M.F., Fredlund, D.G.: Effect of rainfall on matric suction in a residual soil slope. Can. Geotech. J. **33**, 618–628 (1996)
17. Li, X.W., Kong, L.W., Guo, A.G.: Permeability and mechanical characteristics of expansive and cut slope protection mechanism under vegetation action. Rock Soil Mech. **34**, 85–91 (2013)
18. Chen, J.L., Li, J.H., Cheng, P., Song, L., Zhou, T.: Field test on seepage performance of soil cover with different type of vegetation. Rock Soil Mech. **39**, 222–228 (2018)
19. Gabrm, A., Akran, M., Taylor, H.M.: Effect of simulated roots on the permeability of silty soil. Geotech. Test. J. **18**(1), 112–115 (1995)

20. Gallipoli, D., Wheeler, S.J., Karstunen, M.: Modelling the variation of degree of saturation in a deformable unsaturated soil. Géotechnique **53**, 105–112 (2003)
21. Huat, B.B.K., Ali, F.H.J., Low, T.H.: Water infiltration characteristics of unsaturated soil slope and its effect on suction and stability. Geotech. Geol. Eng. **24**, 1293–1306 (2006)
22. Aravena, J.E., Berli, M., Ghezzehei, T.A., Tyler, S.W.: Effects of root-induced compaction on rhizosphere hydraulic properties – X-ray microtomography imaging and numerical simulations. Environ. Sci. Technol. **45**, 425–431 (2011)
23. Guo, N., Yang, X.H., Chen, Z.H., Gao, D.H., Lai, C.J.: Influence of metrical suction on strength and deformation characteristics of unsaturated loess in intact form. J. Lanzhou Univ. Technol. **43**, 120–125 (2017)
24. Song, H.J., Li, J.Z., Ge, Y.M.: Research on the effects of matric suction on shear strength of unsaturated reticulate red clay. Ind. Constr. **47**, 7–11 (2017)
25. Ng, C.W.W., Ni, J.J., Leung, A.K., Zhou, C., Wang, Z.J.: Effects of planting density on tree growth and induced soil suction. Géotechnique **66**, 711–724 (2016)
26. Xu, W.N., et al.: Technical research of vegetation restoration in disturbance area of hydropower project. Science Press, Beijing (2017)
27. Garg, A., Leung, A.K., Ng, C.W.W.: Comparisons of soil suction induced by evapo-transpiration and transpiration of S heptaphylla. Canadian Geotech. J. **52**, 2149–2155 (2015)
28. Xia, Z.Y., Liu, Q., Xu, W.N., Rao, Y.K., Zhang, H.: Characteristics of interface friction between Indigofera amblyantha root system and soil. J. Soil Water Conserv. **32**, 128–134 (2018)
29. Brooks, R.H., Corey, A.T.: Hydraulic properties of porous media. Hydrological Paper **3**, 27 (1964)
30. Van-Genuchten, M.T.: A closed-from equation for predicting the hydraulic conductivity of unsaturated soils. Soil Sci. Soc. Am. J. **44**, 892–898 (1980)
31. Fredlund, D.G., Xing, A.: Equations for the soil-water characteristic curve. Can. Geotech. J. **31**, 521–532 (1994)
32. White, N.F., Duke, H.R., Sunada, D.K., Corey, A.T.: Physics of desaturation in porous materials. J. Irrig. Drainage Div. **96**, 165–191 (1970)
33. Yan, Y.J., Wen, B.P., Ji, B.X.: Contribution of matric suction to shear strength of un-saturated remoulded loess soils. J. Eng. Geol. **19**, 865–874 (2011)
34. Sivakumar, V.: A critical state framework for unsaturated soil. University of Sheffield, UK (1993)
35. Thu, T.M., Rahardjo, H., Leong, E.C.: Effects of hysteresis on shear strength envelopes from constant water content and consolidated drained triaxial tests. In: 4th International Conference on Unsaturated Soils (2006)
36. Xiao, J.H., Liu, J.K., Peng, L.Y., Chen, L.H.: Effects of compactness and water Yellow River alluvial silt content on its mechanical behaviors. Rock Soil Mech. **29**, 409–414 (2008)
37. Peng, L.Y., Liu, J.K., Chen, L.H.: Strength and yielding characteristics of unsaturated compacted silts. Rock Soil Mech. **29**, 2241–2245 (2008)
38. Wang, G.Y., Li, B., Luo, J., Fu, H.Y.: Study of soil-water characteristics and matric suction measurement device for unsaturated silty soil. Rock Soil Mechan. **31**, 3678–3682 (2010)
39. Bengough, A.G., Mullins, C.E.: Mechanical impedance to root growth: a review of experimental techniques and root growth responses. Soil Sci. **41**, 341–358 (1990)
40. Lipiec, J., Hakansson, I.: Influences of degree of compactness and matric water tension on some important plant growth factors. Soil Tillage Res. **53**, 87–94 (2000)
41. Leung, A.K., Garg, A., Ng, C.W.W.: Effects of plant roots on soil-water retention and induced suction in vegetated soil. Eng. Geol. **193**, 183–197 (2015)
42. Fredlund, D.G., Morgenstem, N.R., Widger, R.A.: The shear strength of unsaturated soils. Can. Geotech. J. **15**, 313–321 (2002)

43. Baets, S.D., Poesen, J., Gyssels, G., Knapen, A.: Effects of grass roots on the erodibility of topsoils during concentrated flow. Geomorphology **76**, 54–67 (2006)
44. Wei, H.W., Luo, H.B., Zhang, Y.H.: Root distribution characteristics and tensile strength of Cynodon dactylon. Bullet. Soil Water Conserv. **31**(4), 185–189 (2011)
45. Yang, Y.S., Xia, Z.Y., Xiao, H., Jia, F.G., Hu, M.Z., Deng, L.: Experimental research on shear strength of Indigofera amblyantha root-soil composite. J. Yangtze River Sci. Res. Inst. **31**, 72–76 (2014)
46. Jackson, R.B., Mooney, H.A., Schulze, E.D.: A global budget for fine root biomass surface area and nutrient contents. Proc. Natl. Acad. Sci. USA **94**, 7362–7366 (1997)